Atmospheric Research 242 (2020) 104984

Contents lists available at ScienceDirect

Atmospheric Research

journal homepage: www.elsevier.com/locate/atmosres

Impact of future loss of glaciers on precipitation pattern: A case study from south-eastern Tibetan Plateau

Liying Ren, Keqin Duan*, Rui Xin

Shaanxi Normal University, Xi'an, China

ARTICLE INFO

Keywords:
The Tibetan plateau
Glaciers
Precipitation
WRF model
Climate change

ABSTRACT

Thousands of glaciers in the south-eastern Tibetan Plateau (SETP) are retreating rapidly, which would significantly change land surface properties and lead to intended climate consequences. Results of our study, backed by Weather Research and Forecasting (WRF) Model, suggest the glaciers loss could lead to reorganization of local convection. The glaciers could have inhibited the northward warmer Indian monsoon flow by the downward glacier wind. While, in the absence of glaciers, as the cooling effect of glacier disappears, the original glacier area becomes a heating source and the downhill glacial wind turns to uphill wind, which strengthens the transportation of warm moist air to the highlands, causing more than 20% precipitation in the high elevation area, in the SETP. We conclude that glacier loss, expected in the next decades, could substantially impact the precipitation pattern in the SETP, thus highlighting another mechanism by which human-caused climate change could change future water resource of the Brahmaputra River.

1. Introduction

The Tibetan Plateau (TP) is one of the most vulnerable regions in the world to temperature rise, due to its widespread mountain glaciers (Sha et al., 2015; Yao et al., 2015). Glaciers have the characteristics of surface temperature less than 0 °C and high albedo, hence, they play a crucial role in regulating climate. Similar to the water tower of Asia (Xu et al., 2008), the deglaciation on the TP is responsible for local hydrology cycle variation and consequent impacts on water availability (Immerzeel et al., 2010; Natalie et al., 2008), attracting many researchers to explore the response of glacier variability to climate change (Wang et al., 2017; Wang et al., 2011). Over the past several decades, the temperature in the TP has dramatically increased (Guo and Wang, 2012; Guo et al., 2016) and reached the highest temperature in 2016, leading to significant mass deficit of glaciers (Bolch et al., 2012; Yao et al., 2012). So far, several studies have predicted that the climate in the TP will continue to warm over the next decades (You et al., 2019; Zhou et al., 2014), which results in disappearing most of the glaciers by the end of 2100 in RCP2.6 and RCP4.5 (Zekollari et al., 2019).

As the fastest deglaciation region on the TP, the south-eastern Tibetan Plateau (SETP) is one of the glacier centers in the TP, holding more than 6000 marine glaciers, with a total area of 9470 km^2 (Fig. 1) (Shi et al., 2008). The SETP is mainly controlled by the Indian monsoon circulation, which transports abundant moist and warm air from Indian Ocean to this region. Both the abundant water vapor and high elevation maintain the presence of glaciers in the SETP. The glacier in the SETP is very sensitive to climate warming (Bolch et al., 2010), indeed, at the glacier equilibrium line altitude, the summer temperature is 1–5 °C and the ice temperature is −1–0 °C (Shi and Liu, 2000), which means that only a slight temperature rise could cause a significant glacier ablation in the SETP. A recent study on the glaciers in the SETP suggests that the glaciers have retreated and thinned dramatically in the past decades, with the decreasing rate in mass balance of −0.76 m w.e. per year, during the period of 2003–2010 (Yang et al., 2016). Some glaciers, such as the Baishui No.1 glacier in the SETP, have already lost their accumulation area, indicating accelerating ablation of glaciers (Du et al., 2015). The projection shows that the accumulation areas of some glaciers in the SETP have been already lost and others will be lost in the next few decades, under the RCP4.5 scenario (Duan et al., 2017).

Under the condition of the present global warming, the glaciers in the SETP will be disappeared, during the next few decades. However, only few studies have considered the glacier loss as a possible cause of precipitation variation over the SETP. Theoretically, physical mechanism involves surface warming over the newly free glacier areas, which in turn drives local circulation by perturbing convection patterns. Although this mechanism has not been considered as a primary driver of SETP's precipitation variability, scientific interest in the "glacier loss hypothesis" has been heightened by the extremely glacier

* Corresponding author.
E-mail addresses: renly@snnu.edu.cn (L. Ren), kqduan@snnu.edu.cn (K. Duan).

https://doi.org/10.1016/j.atmosres.2020.104984
Received 8 January 2020; Received in revised form 28 February 2020; Accepted 2 April 2020
Available online 03 April 2020
0169-8095/

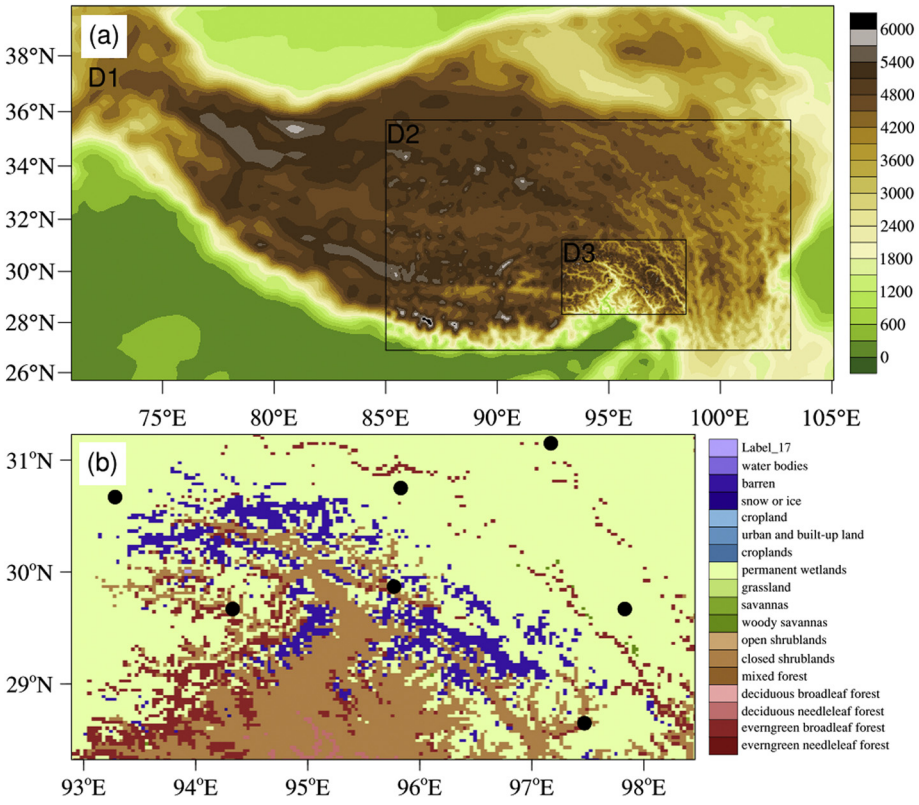

Fig. 1. (a) Simulation domain and topography distribution (units:m), (b) the land use in domain 3. The blue colour represents snow and ice and the black spots represent the location of Meteorological stations. (For interpretation of the references to colour in this figure legend, the reader is referred to the web version of this article.)

retreat, expected in the 21st century. Motivated by this idea, this study aims to focus on identifying the possible mechanisms by which the precipitation in the SETP could be affected by the glacier loss. As a novel feature of our approach, we simulate the precipitation pattern in glacier cover in 2017 over the SETP as the control simulation and design a sensitivity simulation with glacier-free assumption. Subsequently, the comparison between two simulations, i.e. with-glacier and without-glacier simulations, allows us to identify the precipitation response to the glacier loss.

2. Data and methods

2.1. Experiments design

The Weather Research and Forecast Model (WRF, http://www2.mmm.ucar.edu) has been employed to simulate the pattern of precipitation over the SETP. The new version of the model, i.e. WRF3.9.1, overcomes the shortcomings of coarse re-analysis data, which failed to capture complex terrain rainfall modes accurately (Jesse et al., 2017). The WRF3.9.1 has been widely used in mountainous regions, including the TP (Gao et al., 2015; Lin et al., 2018; Tian et al., 2017).

To detect the impact of glacier on precipitation variability, using the WRF model, two sets of experiments are designed, including with (control) and without (sensitivity) glaciers experiments. In the control experiment, the 2013 MODIS in summer land cover types products -MCD12Q1 dataset (Friedl and Sulla-Menashe, 2019) with the spatial resolution of 500 m is used. While, in the sensitivity experiment, the glacier and snow in the land data is replaced by barren. In addition to the changes in the underlying surface of the glacier in the land use, the same experimental setup and physical process parameter scheme are used in the two sets of experiments. Subsequently, the difference between the control and the sensitivity tests are identified to reflect the potential impact of the glacier in the SETP on the regional precipitation. In the model, the ice and snow converge area is 12,870 km^2, while, the actual glacial area in the area is 9470km^2, with a small proportion of snow.

Fig. 1a shows the simulation domain, which uses three layers of one-way nested domains, including D1(120 × 60 grid cells), D2(190 × 109 grid cells), and D3(190 × 109 grid cells), with the resolution of 27 km, 9 km, and 3 km, respectively. Fig. 1b represents the land use in the domain D3. Followed by Maussion et al. (2011), The physical parameter schemes are set. Physical packages include the Modified Thompson microphysics scheme (Thompson et al., 2008), the New Grell–Devenyi 3 Cumulus parameterization scheme (Grell and Dévényi, 2002) (except for D3), the Noah land-surface model (Chen and Dudhia, 2001), the Mellor–Yamada–Janjic TKE planetary boundary layer (PBL) scheme (Janić, 2001), the Rapid radiative transfer model (RRTM) for long-wave radiation (Mlawer et al., 1997), and the Dudhia scheme for Short-wave radiation (Dudhia, 1989). Among them, the land surface model (LSM) is ideal for simulation, as the LSM in the WRF markedly changes circulation patterns in the lower troposphere over the Himalaya and the different treatments of snowpack are remarkable between the schemes. This model is used in this study, since it may affect the orientation, location, and magnitude of moisture transport into the mountains (Thomas et al., 2014). In comparison with other LSMs, the Noah-MP LSM more accurately simulates terrestrial moisture processes and the evolution of snowpack on the timescale of months (Niu et al., 2011). The simulation time spans a mature summer monsoon period from 00:00 UTC on 1 May 2017 to 00:00 UTC on 1 September 2017. The first 31 days are used only for spin-up and are not applied in the analysis. The D1 initial and lateral boundary conditions are configured with the global reanalysis data FNL, provided by the NCEP, with a spatial resolution of 1° × 1° and a temporal interval of 6 h (https://rda.ucar.edu).

2.2. Precipitation data for model comparison

The controlled simulation precipitation is compared with the products of the global precipitation measurement mission (GPM). The GPM offers a new generation of the global monthly precipitation and snow

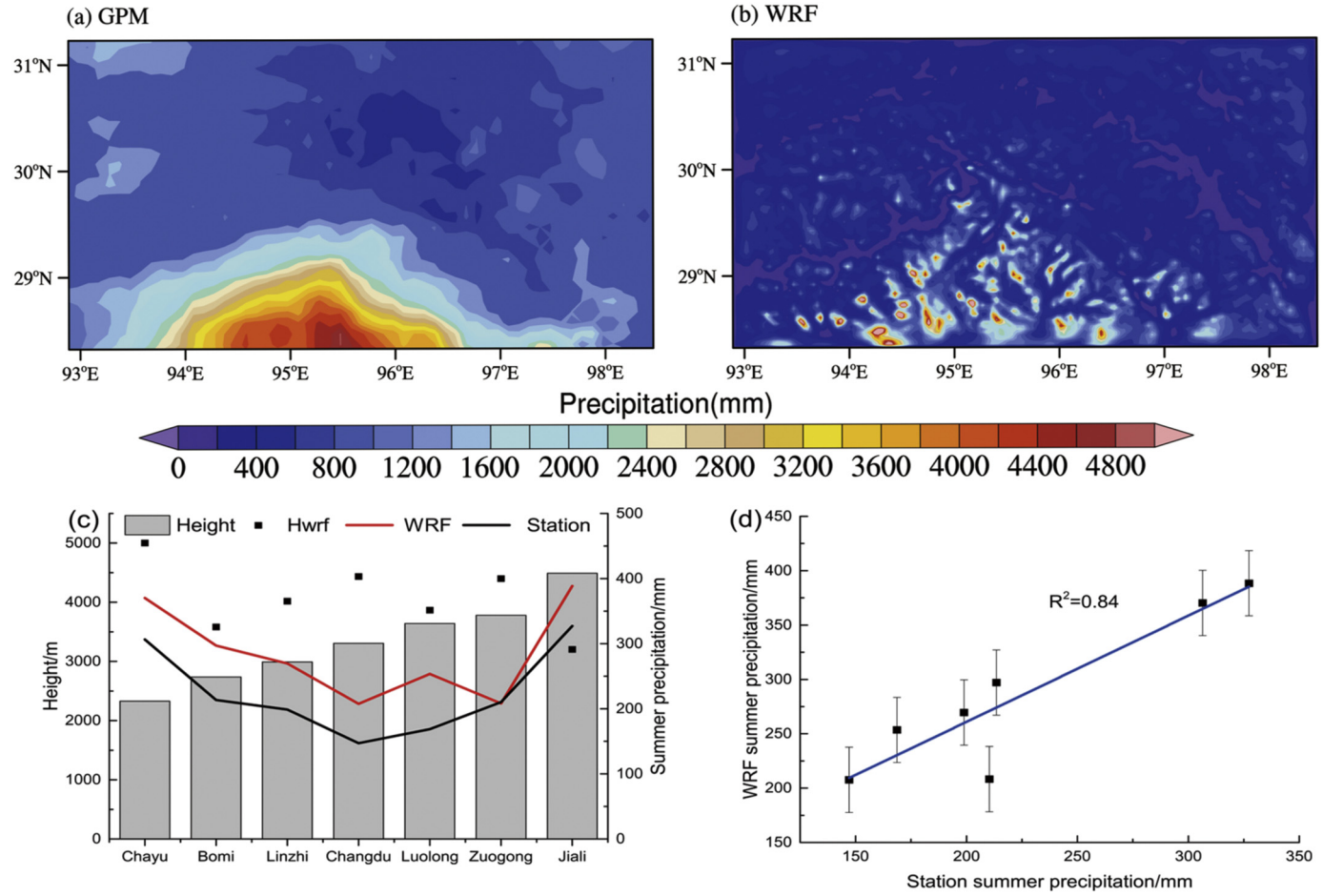

Fig. 2. (a) Spatial pattern of summer precipitation for the GPM over the SETP, (b) Spatial pattern of summer precipitation for the WRF over the SETP, (c) Comparison of station observations with the corresponding grid model simulations, (d) Correlation coefficient of station observations and the corresponding grid model simulations. Gray bar in (c) indicates the station altitude and the Hwrf depicts the mean elevations of the 9 grid points corresponding to the stations.

products, with the spatial resolution of 0.1° × 0.1° (https://pmm.nasa.gov/). The precipitation data from the GPM has been proved more reliable, compared to the TRMM (Tropical Rainfall Measuring Mission) in the southern TP (Xu et al., 2017). The simulated precipitation is also compared with the observational data provided by the Chinese National Meteorological Information Center (http://www.nmic.cn/).

3. Results

3.1. Model validation of the precipitation

Fig. 2 represents the summer precipitation patterns of the GPM and the WRF control experiment over the SETP, in 2017. Generally, the pattern of precipitation from the simulation is consistent with that of the GPM. Both patterns reflect the spatial variation of precipitation, due to the undulating terrain. Compared to the GPM data with resolution of about 10 km, the WRF simulation with finer resolution of 3 km shows more details of precipitation variation with terrain. The highest precipitation mainly concentrates in the trumpet region of the Brahmaputra River, with an altitude below 3000 m. While, the precipitation significantly decreases to less than 400 mm over the plateau region with altitude more than 3000 m.

Fig. 2c provides further comparisons between the seven meteorology observations, with corresponding average simulated precipitation of 9 grid points, surrounding the stations. Both the simulation and observation vary with altitude, in the same way. The correlation coefficient of the two data is 0.91($P < .01$) in Fig. 2d. However, the WRF simulated precipitation is higher than the station observations, probably caused by complex terrain in the SETP, producing more precipitation in the simulation by enhancing the uplift of small and medium-scale terrain. Meanwhile, the altitude of model grid is different from that of stations (Fig. 2c). Despite this uncertainty, the WRF simulation is reliable for the precipitation in the SETP and can be used to detect the impact of glacier on the local precipitation.

3.2. Impact of glacier loss on precipitation

Fig. 3a illustrates the differences of precipitation pattern between the sensitivity and control simulations ("Noglacier"-"Glacier", Same as below). The main disagreements between the two simulations occur in the glacial region and the low-altitude trumpet zone of Brahmaputra River. As the glaciers disappear, the precipitation is likely to increase by 20%–50% in the high elevation region, i.e. the areas with altitude more than 3000 m a.s.l, especially in the original glacier region. The largest increment could be over 400 mm, which is almost twice of the original in the glacier region. In contrast, the precipitation in the low-elevation area in the south side of the glacier reduces by about 20%, with the largest decrease of more than 200 mm. Therefore, the glaciers in the SETP have a strong impact on the local precipitation, in the study area.

Fig. 3b demonstrates the meridional precipitation profiles of both simulations along 96°E. Generally, the precipitation is correlated with the topography and decreases dramatically with the increase of elevation. The precipitation peaks and valleys correspond to the mountain peaks and valleys, respectively. Several precipitation peaks, up to

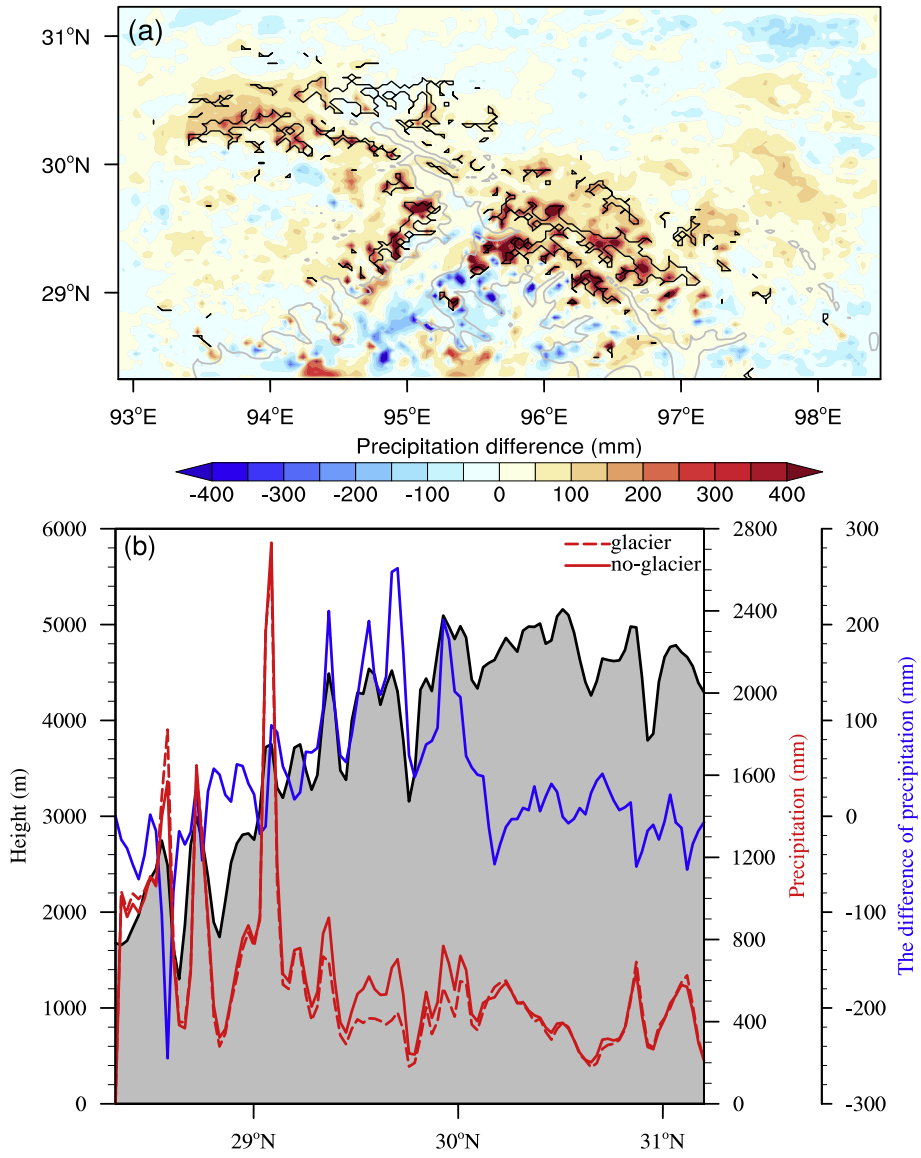

Fig. 3. The difference of summer precipitation between sensitivity and control experiments: (a) in the SETP and (b) along 96°E profile ("Noglacier"-"Glacier"). The gray curves represent isoheight of 3000 m a.s.l and the black curve represents glacier boundary in the SETP.

2400 mm, occur at the elevation between 2500 and 3500 m in the south slope of the SETP, which is due to the blocking effect of the TP on the northward warm and moist air flow during summer. Furthermore, the precipitation on the windward slope of the plateau is much larger than that on the leeward slope.

For the altitude more than 3000 m in the south slope of SETP, the precipitation is higher in the absence of glaciers, compared to the situation when the glacier exists (blue line in Fig. 3b). In contrast, for the altitude lower than 3000 m, the precipitation is generally smaller in the absence of glacier, compared to the situation when the glaciers exist. This phenomenon also exists in other meridional profiles. This indicates that the existence of glaciers reduces the precipitation at high elevation (i.e. altitude more than 3000 m a.s.l) in the south slop of the SETP, also, it is expected that the precipitation pattern in SETP would change, when the glaciers disappear.

3.3. Atmospheric processes associated with the impact of glacier loss on precipitation

The difference of precipitation between the two experiments can be plausibly related to the water vapor flux (WVF), as WVF is the major water vapor source for precipitation over the TP in summer (Zhang et al., 2017). The average summer WVF from the south to the north of the SETP is presented in Fig. 4a. In summer, the tropical marine air masses, carried by the Indian monsoon, move northward to the TP and the WVF can reach up to 240 $kg{\cdot}m^{-1}\ s^{-1}$, in the low altitude region (< 800 m a.s.l) of the Brahmaputra valley. While, at high altitude (i.e. more than 4000 m a.s.l), the WVF significantly decreases, reaching to less than 150 $kg{\cdot}m^{-1}\ s^{-1}$, which is due to the increase in terrain height that hinders the WVF transport northward.

The difference of summer WVF between the sensitivity and control simulations is presented in Fig. 4b. The WVF increases more than 30 $kg{\cdot}m^{-1}\ s^{-1}$ over the original glacier region, indicating the existence of glaciers inhibit the WVF to the highlands over the SETP and tend to concentrate water vapor in the low altitude valley. Thus, more precipitation happens in the low altitude area in the southern slope of the SETP. Conversely, in the case of the glacier disappearance, more water vapor could be transported northward to the higher altitudes, causing more precipitation in the original glacier area. To further investigate the responses of the WVF to the glacier loss, the meridional surface wind speed and total column water vapor content (two separate items of WVF computation) differences between sensitivity and control

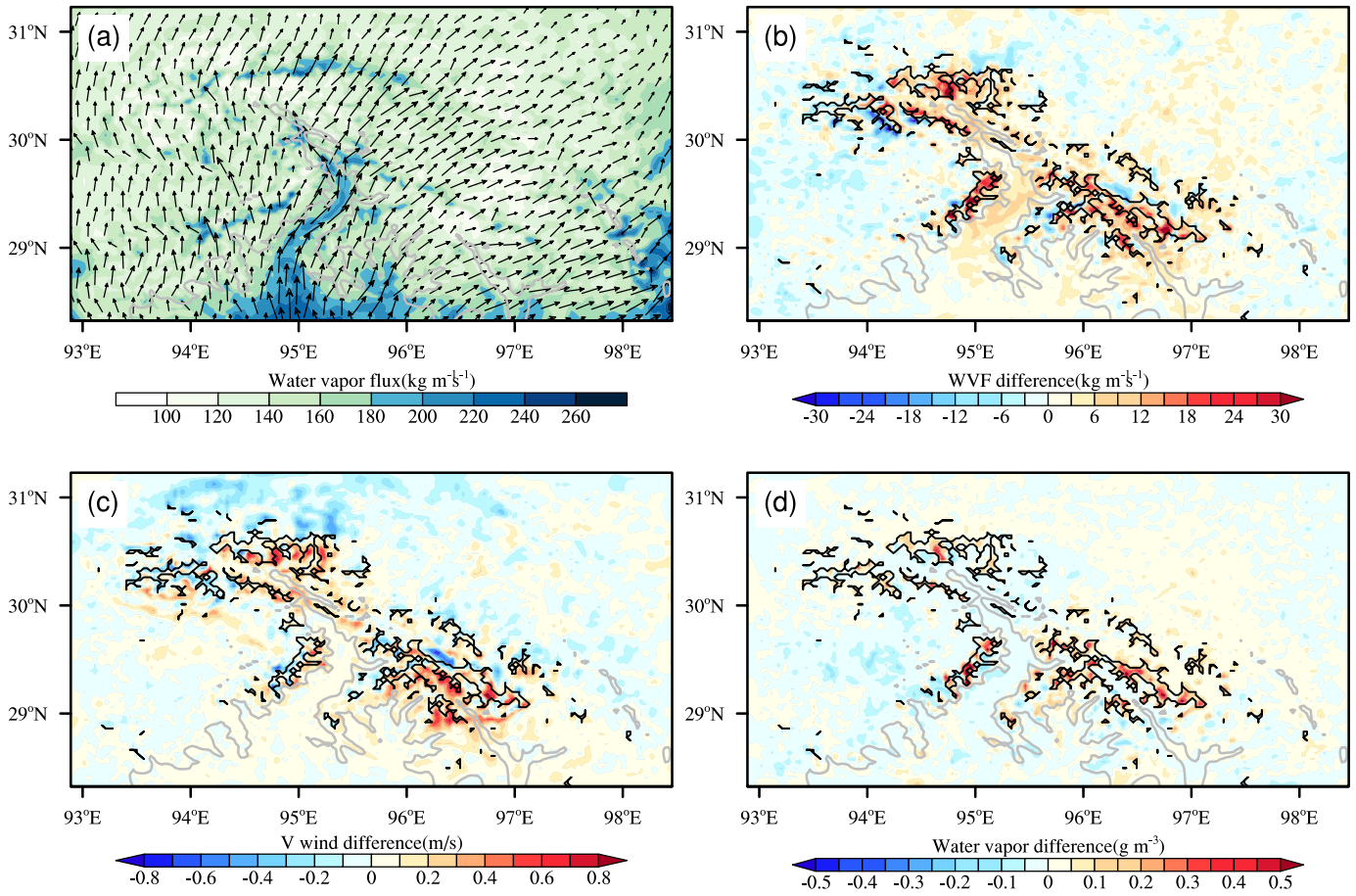

Fig. 4. (a) Spatial pattern of total column water vapor flux. The difference of (b) water vapor flux, (c) the surface meridional wind speed, and (d) the total column water vapor content between the sensitivity and control experiments. The gray curves represent the isoheight of 3000 m a.s.l and the black curve represents the glacier boundary.

simulations are also demonstrated in Fig. 4c and d, respectively. As the glacier disappearance, the south meridional surface wind speed will increase (decrease) in the south (north) slope of the SETP. While, the total column water vapor content will increase dramatically in the original glacier region, indicating that the glaciers cause the atmosphere over the glacier surface to be drier and decrease the northward surface wind.

To evaluate the impacts of the glacier loss on the WVF, we detected the WVF difference between the sensitivity and control experiments, in vertical levels along 96°E profile. As shown in Fig. 5, the strong changes in the WVF mainly occur in the boundary layer with depth of about 1500 m. In the absence of glaciers, vertical wind increases over the original glacier area. Meanwhile, the northward wind along the southern slop of the SETP strengthens, as well. Thus, convection in the boundary layer would be reorganized in the condition of glacier loss, which would guide warm and moist monsoonal air flow moving towards the higher elevation.

3.4. A mechanism scheme of the impact of glacier loss on precipitation change

In summary, combined with Figs. 3 to 5, the mechanism scheme of the impact of glaciers on precipitation is illustrated in Fig. 6. Generally, the glacier surface is a negative sensible heating source to its upper atmosphere, making the atmosphere over the glacier cooler and drier, compared to the situations when the glacier surface is not existed. Thus, as shown in Fig. 6a, the cold, dense air flows downhill, under the force of gravity. This downward glacier wind meets the upward warmer

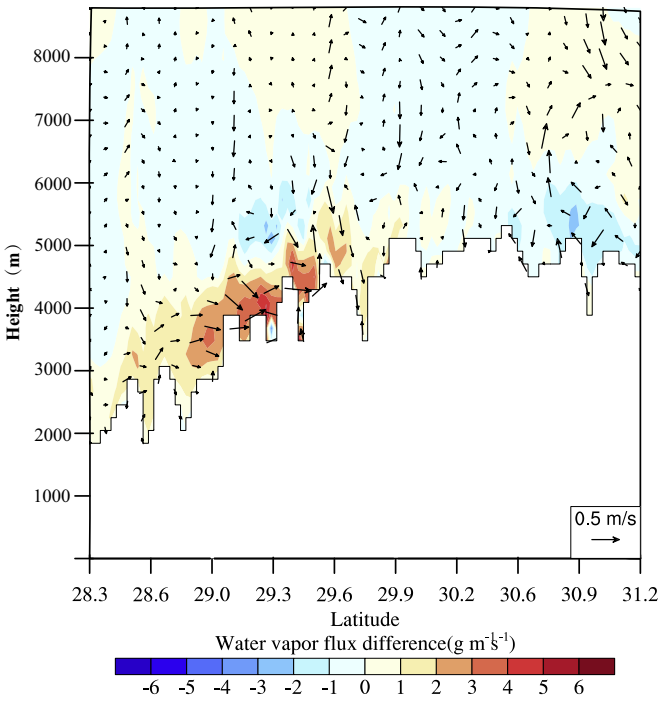

Fig. 5. The difference of meridional wind and water vapor flux between the sensitivity and control experiments, along 96°E profile. The arrow represents meridional-vertical wind speed.

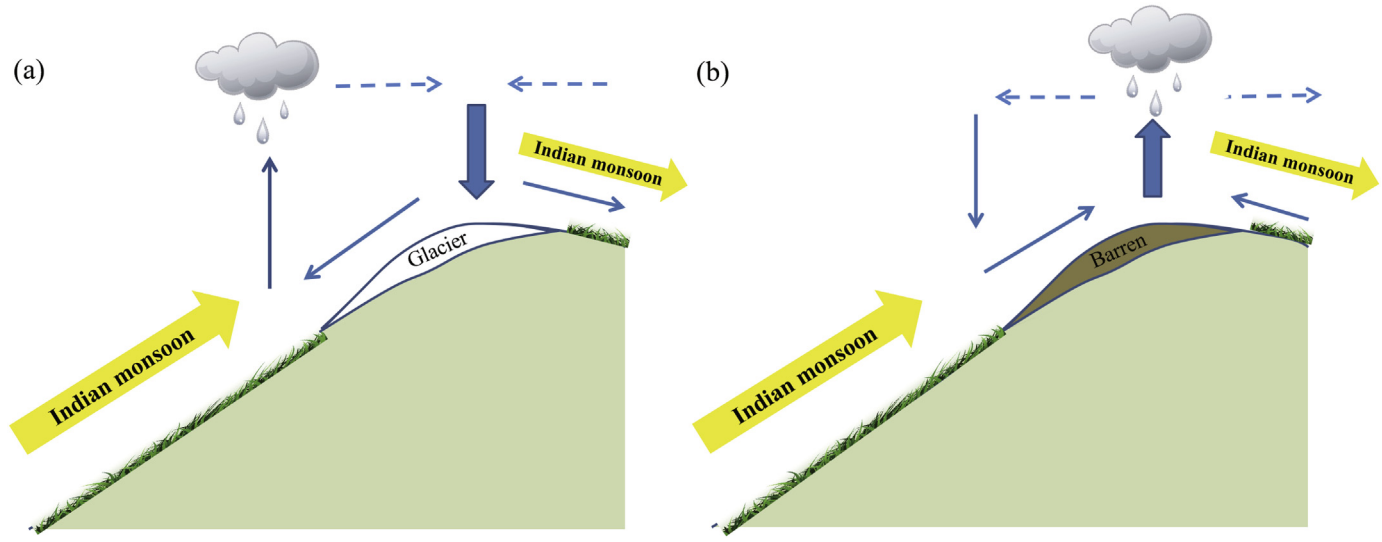

Fig. 6. Schematic diagrams of the main results, presented by the model simulations: (a) in presence of glaciers, (b) in absence of glaciers. Yellow arrows indicate the Indian Monsoon and blue arrows represent the wind direction in the local circulation. (For interpretation of the references to colour in this figure legend, the reader is referred to the web version of this article.)

monsoon air flow in summer, forcing the warmer air to rise and producing more precipitation in the glacier downhill in the south slope of the SETP. Thus, the presence of glaciers is inclined to obstacle the monsoonal flow, climbing over the glaciers. This result is consistent with previous findings, suggesting that glacier delays the moist air, blowing upward and weakens water vapor transportation to the glacier area by analyzing cloud water content (Zhang et al., 2015). Hence, the glaciers can affect the local climate through adjustment of the atmospheric circulations.

When the glaciers are disappeared, the simulated temperature in the original glacier area will rise about 3 °C, through absorbing more solar energy, making the original glacier area as a heat source to its upper atmosphere. Thus, the warmer air over the original glacier region tends to rise and produces a local circulation contrary to the downward glacial wind. In this situation, as presented in Fig. 6b, the monsoonal flow is strengthened in the south slope of the SETP and could transport more water vapor to the higher elevation along the windward slope, making more water vapor over the glacier-free region (Fig. 4b). Therefore, the precipitation in the original glacier area with high altitude will increase, while, the precipitation in the front section of glacier will decrease, as shown in Fig. 3a.

The local circulation can also explain the reason of decreasing the surface wind speed and water content in the northern slope of the glacier (Figs. 4 and 5). In presence of the glaciers, the direction of downward glacier wind in the north slope of the glacier coincides with the monsoonal air flow, strengthening the northward wind. While, in the absence of glaciers, the wind direction of the local circulation in the north slope of the glaciers is opposite to the monsoonal flow, decreasing the northward wind.

4. Conclusions

Simulating future changes in the precipitation pattern is of great importance for industry and agriculture to maintain a sustainable water resource, especially in dense population areas, such as the northeastern India and Bangladesh. As the main river in these areas, Brahmaputra River acquires the major runoff from the SETP, which is one of the glaciated areas in middle latitude region. However, the glaciers in this area are rapidly retreating as a result of global warming and a significant glacier mass loss is expected in the next few decades, which can affect the precipitation pattern in the area. To explore the potential impact of glacier extinction on local precipitation in the SETP, two sets of experiments, including in presence of glacier (control) and in absence of glacier (sensitivity) are designed, using the WRF3.9.1 model, with a resolution of 3 km. Sensitivity test indicates that the presence of glaciers weakens the northward monsoonal air flow, due to the southward downhill glacier wind, resulting in the decrease of water vapor flux in the glacier region. Based on the free-glacier scenario, as the cooling effect of glacier disappears, the original sinking air flow turns to ascending flow and the downhill glacier wind transforms to the uphill wind. This reorganization convection strengthens the northward surface wind, along the south slope of the SETP, which leads to the enhancement of water vapor transport to the higher elevation. Consequently, precipitation would increase by 20–50% at the high altitude and decrease by 20% in the low altitude. Thus, with disappearance of glaciers, caused by global warming, the precipitation in the high altitude will increase, resulting in enhancement runoff in the upper reaches of the Brahmaputra River.

Declaration of Competing Interest

The authors declare that they have no known competing financial interests or personal relationships that could have appeared to influence the work reported in this paper.

Acknowledgments

This research is jointly supported by the Second Tibetan Plateau Scientific Expedition and Research (STEP) program (Grant No. 2019QZKK0201), National Natural Science Foundation of China (Grant No. 41571062), and the Fundamental Research Funds for the Central Universities (Grant No. 2019CSLZ007). The authors would like to thank the anonymous reviewers and editors for their constructive suggestions on the manuscript. MODIS land cover types products for this paper are available at the Land Processes Distributed Active Archive Center (https://lpdaac.usgs.gov/products/mcd12q1v006/). Meteorology observation data are available from the Chinese National Meteorological Information Center (http://www.nmic.cn/). We acknowledge the NCEP Reanalysis data set, obtained from https://rda.ucar.edu and the GPM Data set from https://pmm.nasa.gov/. The WRF simulated results are stored at https://figshare.com/articles/glacier/9783062 and https://figshare.com/articles/ noglacier/9783080 website. Alternatively, please contact the corresponding author (kqduan@snnu.edu.cn).

References

Bolch, T., Yao, T., Kang, S., 2010. A glacier inventory for the western Nyainqentanglha Range and the Nam Co Basin,Tibet,And glacier changes 1976–2009. Cryosphere 4 (3), 419–433. https://doi.org/10.5194/tc-4-419-2010.

Bolch, T., Kulkarni, A., Kääb, A., Huggel, C., Paul, F., Cogley, J., et al., 2012. The state and fate of Himalayan glaciers. Science. 336 (6079), 310–314. https://doi.org/10.1126/science.1215828.

Chen, F., Dudhia, J., 2001. Coupling an advanced land surface-hydrology model with the Penn State-NCAR MM5 modeling system. Part I: model implementation and sensitivity. Mon. Weather Rev. 129 (4), 569–585.

Du, J., He, Y., Li, S., Wang, S., Niu, H., 2015. Mass balance of a typical monsoonal temperate glacier in Hengduan Mountains Region(in Chinese). Acta Geograph. Sin. 70 (9), 1415–1422. https://doi.org/10.11821/dlxb201509005.

Duan, K., Yao, T., Shi, P., Guo, X., 2017. Simulation and prediction of equilibrium line altitude of glaciers in the eastern Tibetan Plateau (in Chinese). Sci. Sin. Terrae 47, 104–113. https://doi.org/10.1360/N072016-00062.

Dudhia, J., 1989. Numerical study of convection observed during the winter monsoon experiment using a mesoscale two-dimensional model. J. Atmos. Sci. 46 (20), 3077–3107.

Friedl, M., Sulla-Menashe, D., 2019. MCD12Q1 MODIS/Terra + aqua land cover type yearly L3 global 500m SIN grid V006 [Data set]. NASA EOSDIS Land Process. DAAC. https://doi.org/10.5067/MODIS/MCD12Q1.006.

Gao, Y., Xu, J., Chen, D., 2015. Evaluation of WRF mesoscale climate simulations over the Tibetan Plateau during 1979–2011. J. Clim. 28 (7), 2823–2841. https://doi.org/10.1175/JCLI-D-14-00300.1.

Grell, G.A., Dévényi, D., 2002. A generalized approach to parameterizing convection combining ensemble and data assimilation techniques. Geophys. Res. Lett. 29 (14). https://doi.org/10.1029/2002GL0153.

Guo, D., Wang, H., 2012. The significant climate warming in the northern Tibetan plateau and its possible causes. Int. J. Climatol. 32 (12), 1775–1781. https://doi.org/10.1002/joc.2388.

Guo, D., Yu, E., Wang, H., 2016. Will the Tibetan Plateau warming depend on elevation in the future? J. Geophys. Res.-Atmos. 121, 3969–3978. https://doi.org/10.1002/2016JD024871.

Immerzeel, W.W., van Beek, L.P.H., Bierkens, M.F.P., 2010. Climate Change Will Affect the Asian Water Towers. Science 328 (5984), 1382–1385. https://doi.org/10.1126/science.1183188.

Janić, Z.I., 2001. Nonsingular Implementation of the Mellor-Yamada Level 2.5 Scheme in the NCEP Meso Model, Technical Report, National Centers for Environmental Prediction. Office Note No. 437.

Jesse, N., Leila, M.V., Charles, J., Forest, C., Bodo, B., Elisa, P., 2017. The spatiotemporal variability of precipitation over the Himalaya: evaluation of one-year WRF model simulation. Clim. Dyn. 49, 2179–2204.

Lin, C., Chen, D., Yang, K., Ou, T., 2018. Impact of model resolution on simulating the water vapor transport through the Central Himalayas: implication for models' wet bias over the Tibetan Plateau. Clim. Dyn. 51 (9–10), 3159–3207.

Maussion, F., Scherer, D., Finkelnburg, R., Richters, J., Yang, W., Yao, T., 2011. WRF simulation of a precipitation event over the Tibetan Plateau, China—an assessment using remote sensing and ground observations. Hydrol. Earth Syst. Sci. 15 (6), 1795–1817.

Mlawer, E.J., Taubman, S.J., Brown, P.D., Iacono, M.J., Clough, S.A., 1997. Radiative transfer for inhomogeneous atmospheres: RRTM, a validated correlated-k model for the longwave. J. Geophys. Res.-Atmos. 102 (D14), 16663–16682.

Natalie, M., Lonnie, G., Yao, T., Ellen, M., Ulrich, S., Vasily, A., et al., 2008. Mass loss on Himalayan glacier endangers water resources. Geophys. Res. Lett. 35, L22503. https://doi.org/10.1029/2008GL035556.

Niu, G., Yang, Z., Mitchell, K.E., Chen, F., Ek, M.B., Barlage, M., et al., 2011. The community Noah land surface model with multiparameterization options (NoahMP): 1. Model description and evaluation with localscale measurements. J. Geophys. Res. 116 (D12109), 19.

Sha, Y., Shi, Z., Liu, X., An, Z., 2015. Distinct impacts of the Mongolian and Tibetan Plateaus on the evolution of the East Asian monsoon. J. Geophys. Res.-Atmos. 120 (10), 4764–4782. https://doi.org/10.1002/2014JD022880.

Shi, Y., Liu, S., 2000. Estimation on the response of glaciers in China to the global warming in the 21st century. Chin. Sci. Bull. 45 (7), 668–672.

Shi, Y., Liu, C., Wang, Z., 2008. Concise Glacier Inventory of China. Shanghai Popular Science Press, Shanghai.

Thomas, L., Dash, S.K., Mohanty, U.C., 2014. Influence of various land surface parameterization schemes on the simulation of Western disturbances. Meteorol. Appl. 21, 635–643.

Thompson, G., Field, P.R., Rasmussen, R.M., Hall, W.D., 2008. Explicit forecasts of winter precipitation using an improved bulk microphysics scheme. Part II: implementation of a new snow parameterization. Mon. Weather Rev. 136 (12), 5095–5115. https://doi.org/10.1175/2008MWR2387.1.

Tian, J., Liu, J., Wang, J., Li, C., Yu, F., Chu, Z., 2017. A spatio-temporal evaluation of the WRF physical parameterisations for numerical rainfall simulation in semi-humid and semi-arid catchments of Northern China. Atmos. Res. 191, 141–155.

Wang, W., Yao, T., Yang, X., 2011. Variations of glacial lakes and glaciers in the Boshula mountain range, Southeast Tibet, from the 1970s to 2009. Ann. Glaciol. 52, 9–17.

Wang, Q., Yi, S., Sun, W., 2017. Precipitation-driven glacier changes in the Pamir and Hindu Kush mountains. Geophys. Res. Lett. 44, 2817–2824. https://doi.org/10.1002/2017GL072646.

Xu, X., Lu, C., Shi, X., Gao, S., 2008. World water tower: An atmospheric perspective. Geophys. Res. Lett. 35, L20815. https://doi.org/10.1029/2008GL035867.

Xu, R., Tian, F., Yang, L., Hu, H., Lu, H., Hou, A., 2017. Ground validation of GPM IMERG and TRMM 3B42V7 rainfall products over southern Tibetan Plateau based on a high-density rain gauge network. J. Geophys. Res.-Atmos. 122 (2), 910–924. https://doi.org/10.1002/2016JD025418.

Yang, W., Guo, X., Yao, T., Zhu, M., Wang, Y., 2016. Recent accelerating mass loss of southeast Tibetan glaciers and the relationship with changes in macroscale atmospheric circulations. Clim. Dyn. 47, 805–815. https://doi.org/10.1007/s00382-015-2872-y.

Yao, T., Thompson, L., Yang, W., Yu, W., Gao, Y., Guo, X., et al., 2012. Different glacier status with atmospheric circulations in Tibetan Plateau and surroundings. Nat. Clim. Chang. 2 (9), 663–667.

Yao, T., Wu, F., Ding, L., Sun, J., Zhu, L., Piao, S., et al., 2015. Multispherical interactions and their effects on the Tibetan Plateau's earth system: a review of the recent researches. Nat. Sci. Rev. 2, 468–488. https://doi.org/10.1093/nsr/nwv070.

You, Q., Zhang, Y., Xie, X., Wu, F., 2019. Robust elevation dependency warming over the Tibetan Plateau under global warming of 1.5 °C and 2 °C. Clim. Dyn. 53, 2047–2060.

Zekollari, H., Huss, M., Farinotti, D., 2019. Modelling the future evolution of glaciers in the European Alps under the EURO-CORDEX RCM ensemble. Cryosphere 13, 1125–1146.

Zhang, X., Duan, K., Liu, H., 2015. Study of the cloud structure over the Mount Nyainqêntanglha during summer (in Chinese). Adv. Water Sci. 26 (2), 196–200.

Zhang, C., Tang, Q., Chen, D., 2017. Recent changes in the moisture source of precipitation over the Tibetan Plateau. J. Clim. 30 (5), 1807–1819. https://doi.org/10.1175/JCLI-D-15-0842.1.

Zhou, B., Wen, Q., Xu, Y., Song, L., Zhang, X., 2014. Projected changes in temperature and precipitation extremes in China by the CMIP5 multi-model ensembles. J. Clim. 27, 6591–6611. https://doi.org/10.1175/JCLI-D-13-00761.1.